ChemistrySelect
Research Article
doi.org/10.1002/slct.202104228
Chemistry Europe
European Chemical Societies Publishing
www.chemistryselect.org

Materials Science inc. Nanomaterials & Polymers

Modification of High-Density Polyethylene through the Grafting of Methyl Methacrylate Using RAFT Technique and Preparation of Its Polymer/Clay Nanocomposites**

Mehdi Hosseinzadeh,*[a] Mojtaba Abbasian,[b] Leila Ghodsi,[b] Saber Ghasemi Karaj-Abad,*[b] Metin Hayri Acar,[c] Farideh Mahmoodzadeh,[d] and Mehdi Jaymand[e]

A well-defined method for discovering an easy and effective strategy through graft copolymer derived from poly (methylmethacrylate) (PMMA) as a monomer, high-density polyethylene (HDPE) and its organoclay nanocomposite with physicochemical and mechanical properties was successfully prepared *by* reversible addition-fragmentation transfer (RAFT) polymerization, and factors organoclay (Cloisite® 20 A) on the terminal features of the obtained graft copolymer were investigated. First, maleic anhydride (MA) was grafted onto HDPE directed by, the inauguration of an anhydride chain with ethanolamine to develop a hydroxylated high-density polyethylene (HDPE-OH). After that, the hydroxyl masses were esterified by using RAFT agent, 4-cyano-4-[(phenyl carbon thionyl) sulfanyl valeric acid to obtain HDPE-CTA macroinitiator. Then, the MMA monomer was grafted onto HDPE via the RAFT method to obtain the HDPE-*g*-PMMA graft copolymer. In the end, HDPE-*g*-PMMA/clay nanocomposite by a solution intercalation method was synthesized. The structures of the, copolymer and nanocomposite were studied by Fourier transform infrared spectroscopy, X-ray diffraction, and Transmission electron microscopy (TEM) techniques. It explores for the synthesis of HDPE-*g*-PMMA/clay nanocomposites, disclosed a foliated structure. Based on the thermic behavior, synthesized HDPE-*g*-PMMA/clay nanocomposites can display the above thermic solidity with just some extent (5) of organoclay.

Introduction

Polyethylene (PE) is the most widely thermoplastic that is used among polyolefin's.[1,2] Commonly, it has been applied in industrial and user crops (for example, packaging and tube substances) applications. Even today, the consumption of PE follows it is growing, mainly for the sake of its down cost, excellent chemical resistance, acceptable processability and, mechanical properties, good thermal stability, insulation characteristics, and water resistance.[3–6]

Polyethylene is manufactured in different forms as follows:

a) Linear Polyethylene (LPE)
b) Low Density Polyethylene (LDPE)
c) Ultra-Low-Density Polyethylene (ULDPE)
d) High-Density Polyethylene (HDPE)
e) Ultra-High-Density Polyethylene (UHDPE)
f) Linear Low-Density Polyethylene (LLDPE).[7]

Each of these manufacturers has different usages ranging from packaging, and vessels films for bottles and buckets. Generally, LDPE and LLDPE are chosen for film packaging and electrical insulation. In contrast, HDPE is used for manufacturing household drums, chemical containers and numerous types of industrial packaging, as well as in the piping industry. HDPE and especially UHDPE are the most rigid polymeric materials, which are particularly useful where moisture resistance and low-cost material are required.[8–11] Despite the commercial success of PE, its poor compatibility with dyes, polymers and, fillers, as well as low surface energy and the nonpolar surface, has limited lots of their end-use. To improve these limitations, numerous chemical modification procedures, include incorporation of polar functional groups such as sulfonic acid or succinic anhydride, oxidation (*e.g.*, using ammonium persulphate and nickel sulfate), halogenation, and plasma treatment have often been recognized.[7] Another affections and versatile approach for surface modification of PE are the grafting of other polymers onto the PE backbone.[12–15] The grafting process can be achieved using different strategies, including

---

[a] *Dr. M. Hosseinzadeh*
Marand Faculty of Technical and Engineering,
University of Tabriz,
Tabriz, Iran
E-mail: mh_1268@yahoo.com
[b] *Prof. M. Abbasian, L. Ghodsi, S. G. Karaj-Abad*
Department of Chemistry,
Payame Noor University, P.O. Box: 19395-3697,
Tehran, Iran
E-mail: sg.chemist1988@gmail.com
[c] *Prof. M. H. Acar*
Macromolecular Engineering Research Laboratory,
Chemistry Department, Istanbul Technical University,
Maslak 34469 Istanbul, Turkey
[d] *Dr. F. Mahmoodzadeh*
Halal Research Center of IRI,
FDA, Tehran, Iran
[e] *Dr. M. Jaymand*
Nano Drug Delivery Research Center,
Health Technology Institute,
Kermanshah University of Medical Sciences,
Kermanshah, Iran

[**] *RAFT: Reversible Addition-fragmentation chain Transfer*

Supporting information for this article is available on the WWW under https://doi.org/10.1002/slct.202104228

free-radical initiators, ionizing radiation (electron beam, γ-ray, and X-ray) and, UV radiation.[16–19] The significant problems of these procedures are consist of: little control over the graft operations onto PE backbone, the wide dispensation of molecular weight, a long-lasting modification effect, difficulties in achieving uniform modification, chain depression of PE backbone during the organization of free radical polymerization places, as well as the attendance of it's as a significant of homopolymer in the production.[20–22] For many years, many scholars have the intention to apply reversible impoverished radical polymerization (RIRP) for the synthesis of HDPE-based nanocomposite with well-explanatory structures.[23–25] This attitude is derived into three main classifies, consisting of Nitroxide-mediated radical polymerization (NMRP),[26,27] reversible addition of fragmentation chain transfer (RAFT) polymerization,[28,29] and atom transfer radical polymerization (ATRP),[30,31] which can be used to overcome some of the problems as mentioned above. These methods permit the combination of macromolecules to predetermined thin molecular weight dispensation, useful end-functionalities, and various architectures. Among these, the RAFT method is chiefly noticeable, due to traits of simplicity and suitability to a broad range of vinyl monomers; it's possible to synthesize post-modified polymers, homo-polymers, and amphiphilic graft copolymers with complex macromolecular architectures, controlled molecular weight, and light dispersion.[32,33]

In other words, polymer/clay nanocomposites (PCNs) have received significant consideration in the late few decades. It has been well-established that dispersion of nanoclay in the polymeric matrices subsequently improved mechanical properties, fire retardancy, gas barriers, corrosion resistance, and thermal stability.[34–37] In general, two types of nanocomposites, namely exfoliated and intercalated combinations, can be achieved. During the first combination, the silicate layers are uniformly and steadily, continually scatter in a polymer matrix. During the second combination, macromolecular bonds are placed between silicate layers causing a well-conditioned multilayer morphology to accommodate intermittent inorganic and polymeric layers. This procedure planned for synthesizing of PCNs can be categorized as: (1) solution-blending; (2) *in situ* polymerization; and (3) melt intercalation. Among them, solution-blending shows to be the most efficient and favorable method for the synthesizing of nanocomposites; as a result, it generally leads to homogeneous materials. Also, The adaptability between clay and organic matrix, is a decisive factor for the high loyalty production of PCNs.[38–41] The purpose of this research, is designation, improvement an effective process, and well-developed for the synthesized HDPE-*g*-PMMA by using RAFT method. The polymer/clay nanocomposite of the synthesized graft copolymer was fabricated through a solution intercalation approach. Initially, HDPE was functionalized using MA followed by ethanolamine to produce hydroxylated HDPE (HDPE-OH). The RAFT chain transfer agent (CTA) was immobilized onto the HDPE backbone to afford HDPE-CTA macroinitiator. Then, the MMA monomer was grafted onto the HDPE backbone by the RAFT method to produce a well-developed HDPE-*g*-PMMA grafted copolymer, and to increase the compatibility and adhesion (physicochemical traits) of the consequent copolymer to clay nanoparticles. Finally, HDPE-*g*-PMMA/clay nanocomposites were Successfully synthesized by using a solution intercalation method.

Results and Discussion

As seen in Scheme 1, our primary purpose of this perusal is the amendment of HDPE by grafting of MMA monomer using the RAFT method. Afterward, a small amount (5 wt.%) of silicate layers was combined into the synthesized HDPE-*g*-PMMA graft copolymer to promote physicochemical traits of the final copolymer.

FTIR spectroscopy

The synthesized models, were basically specified by using FTIR spectroscopy. According to Figures 1 and 2, FTIR spectra of the HDPE exhibits the rocking vibration of $-CH_2$ at 730–700 cm^{-1}, bending vibrations of C–H at 1465 and 1376 cm^{-1}, and stretching vibrations of aliphatic C–H at 2920–2800 cm^{-1} region.

The most significant change after grafting of the MA monomer onto HDPE backbone attributed to the symmetrical and asymmetrical stretching ways of anhydride groups in the MA unify, is the manifestation of new absorption bands at 1747 and 1785 cm^{-1}. As shown in FTIR spectra of HDPE-OH, due to reaction with ethanolamine and change to succinimide group,

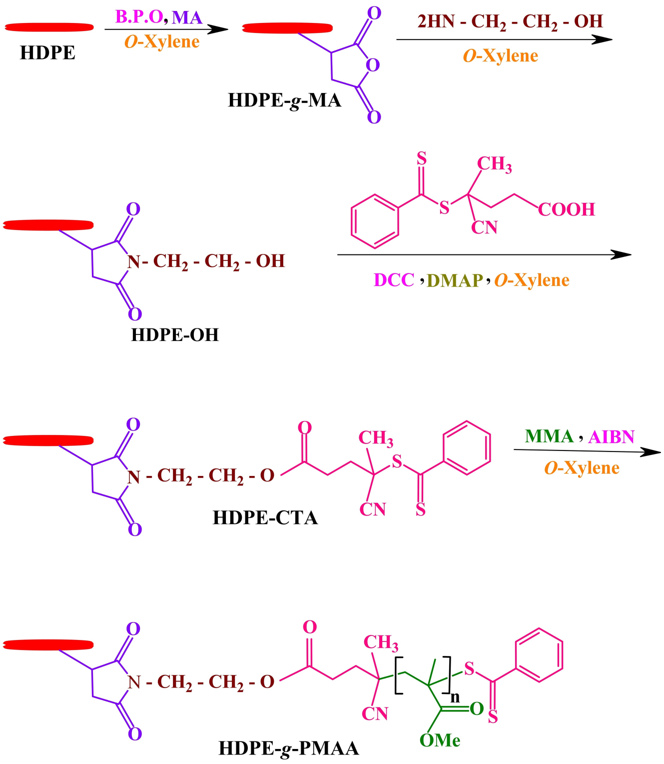

Scheme 1. The overall strategy for the synthesis of HDPE-*g*-PMMA graft coolymer.

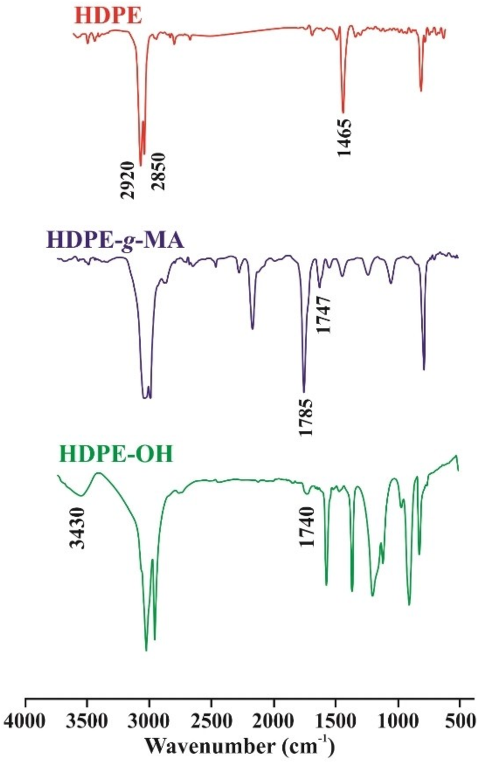

Figure 1. The FTIR spectra of HDPE, HDPE-*g*-MA, and HDPE-OH.

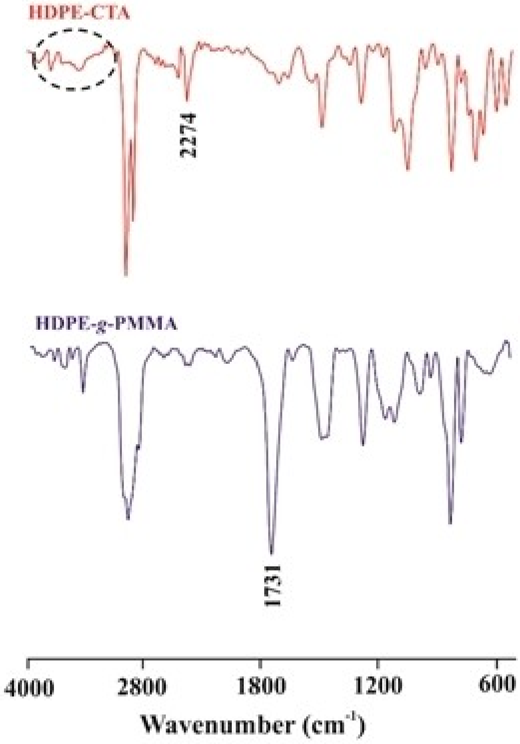

Figure 2. The FTIR spectra of HDPE-CTA, and HDPE-*g*-PMMA.

the absorption bands of anhydride were altered to 1740 cm^{-1}. Also, in this spectrum further significant change that attributed to the hydroxyl group of ethanolamine half, is the advent of hydroxyl stretching vibration as a vast band centered at 3430 cm^{-1} (Figure 1).

Successfully, the synthesis of HDPE-CTA macro-RAFT agent by the invisibility of hydroxyl stretching vibration band at 3430 cm^{-1} was achieved and advent of a new band at 2274 cm^{-1} attributed to cyanide group of RAFT half was confirmed. The successful grafting of the MMA onto monomer by advent of a severe solid was verified. The pointed band at 1731 cm^{-1} is relevant to MMA unifies of the carbonyl group (Figure 2).

Morphology of HDPE-g-PMMA copolymer

The surface morphology of synthesized HDPE-*g*-PMMA copolymer was performed using SEM (Figure 3). As shown, the surface of the sample mainly for the growth of MMA monomer onto HDPE, is partly coarse with some bulges. As well as, the SEM showed a partially homogeneous PMMA attaching onto the functionalized HDPE.

Grafting Reagents

The grafting reagents consisting of grafting efficiency, grafting output, and weight growth for the synthesized HDPE-*g*-MA and HDPE-*g*-PMMA were defined by using of gravimetric approach according to the following equations:

a) Grafting efficiency $(\%GE) = W_g/(W_m + W_0) \times 100$
b) Grafting output $(\%G) = (W_g\text{-}W_0)/W_g \times 100$
c) Weight growth $(\%WG) = (W_g\text{-}W_0)/(W_m + W_0) \times 100$

In these equations, the volume of HDPE-*g*-MA or HDPE-*g*-PMMA, is W_g, the volume of primary HDPE or HDPE-CTA macro-RAFT agent, is W_0 and the volume of MMA or MA monomers taken into consideration for the polymerization is W_m. in Table 1, The grafting reagents were computed and resumed.

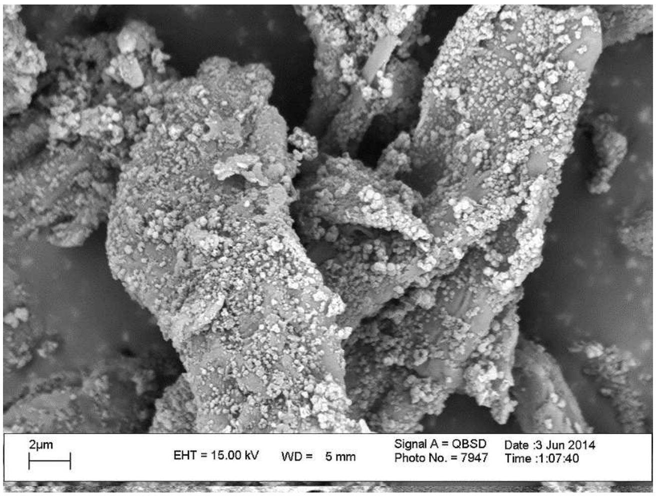

Figure 3. The SEM image of HDPE-*g*-PMMA copolymer.

Table 1. Grafting reagents for the synthesized HDPE-*g*-MA, and HDPE-*g*-PMMA.

Sample	Mass of grafting (W_g)	Weight growth (% WG)	Grafting efficiency (% GE)	Grafting outcome (% G)
HDPE-*g*-MA	6.25	17.8	89.3	20
HDPE-*g*-PMMA	2.30	45.1	80.0	56.5

Characterization of HDPE-g-PMMA/ Cloisite® 20 A nanocomposite TEM and XRD studies

The morphologies and structure of synthesized nanocomposites were considered applying TEM and XRD (Figure 4). Overall, XRD can be used as an effective tool to evaluate the structural kind of, intercalated/or foliated structure and copolymer/clay nanocomposites. An intercalated structure by a reduction in 2 thetas, is defined, indicating of a development in the interlayer areas. But, generally, the formation of a foliated structure between the silicate stratums leads to perfect loss of registry. So, in the XRD pattern, no peak can be seen. Nevertheless, in most cases, an untidy irresolvable system is achieved, that in the XRD pattern shows no refraction peak(s). TEM image in these situations is necessary supplementary documents.[42,43]

The XRD samples of HDPE-g-PMMA/Cloisite® 20 A nanocomposites and Cloisite® 20 A shown in Figure 4. As seen, Cloisite® 20 A showed a refraction peak at 3.68°. Conversely, for the constructed HDPE-g-PMMA/Cloisite® 20 A nanocomposites, as shown in the XRD pattern of this sample, no peak(s) was observed. According to XRD samples and also the above debate, it could be inducted that a foliated or irresolvable structure may be formed for the synthesis of nanocomposites. Further evidence in the structure kind of HDPE-g-PMMA/Cloisite® 20 A nanocomposite was gained using TEM observation. In TEM image, light areas and dark lines, indicate the polymer matrix and silicate stratums, respectively. It should be pointed out that the interactions between polymer and surfactant, also between theirs with clay, have an axial role in the outcome structure. Commonly, an optimized equilibrium of all these interplays leads up to a foliated structure. The TEM micrograph shows a well-scattering of silicate stratums in the HDPE-g-PMMA matrix, and between the silicate stratum, multilayer morphology vanished. This phenomenon determinant a foliated morphology for the HDPE-g-PMMA/Cloisite® 20 A sample according to XRD results.

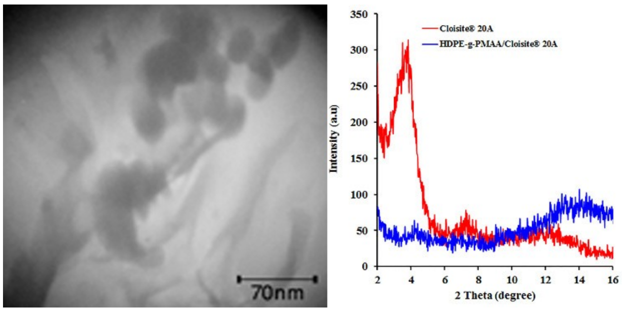

Figure 4. The TEM image of HDPE-g-PMMA/Cloisite® 20 A nanocomposite, and XRD patterns of Cloisite® 20 A and HDPE-g-PMMA/Cloisite® 20 A nanocomposite.

Study of DSC and TGA thermogram

Thermic attributes of pure HDPE, HDPE-g-PMMA, and synthesized nanocomposite were shown in Figures 5 and 6, and investigated by applying DSC and TGA. It is well accepted that both are melting down point (Tm) and glass transition temperature (Tg) of graft copolymer by the side chains have been affected. The random connection of non-crystallizable mono-

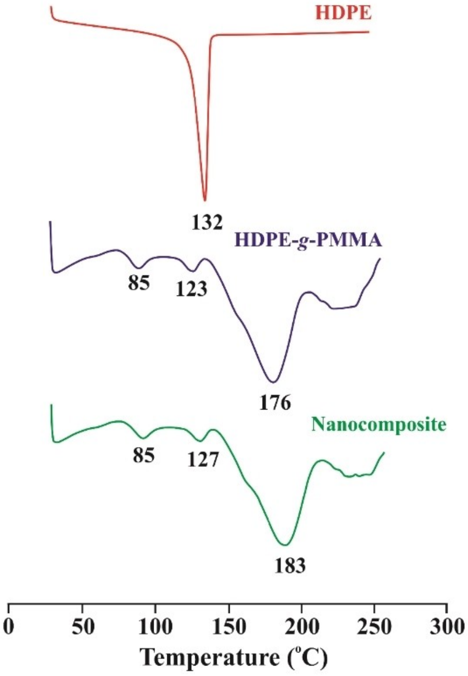

Figure 5. The DSC curves of HDPE, HDPE-*g*-PMMA, and fabricated HDPE-*g*-PMMA/Cloisite® 20 A nanocomposite.

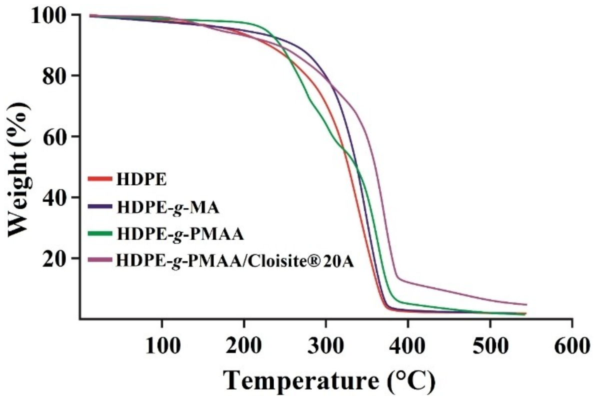

Figure 6. The TGA curves of HDPE, HDPE-g-MA, HDPE-g-PMMA, and synthesized HDPE-g-PMMA/Cloisite® 20 A nanocomposite.

mer units (e.g., MMA) into the backbone of a half-crystalline polymer (e.g., PE) demonstrates the kinetics and thermodynamics result of crystallization. Characteristic DSC curves of HDPE, HDPE-*g*-PMMA, and fabricated HDPE-*g*-PMMA/Cloisite® 20 A nanocomposite are shown in Figure 5.

DSC thermogram of pure HDPE exhibit a solid endothermic top approximately at132 °C corresponding to the amount of thermoplastic Tm. As seen, HDPE did not show any Tg quantity. Conversely, after grafting of MMA monomer onto HDPE, the DSC thermogram has changed considerably. The Tg and Tm values of HDPE-g-PMMA copolymer were obtained as 123 and 176 °C, respectively. This Tg attributed to the motion of PMMA chains, as well as indicator presence of microphage separation in graft copolymer. The resulted separation is for the sake of insolubility of HDPE and PMMA in the polymer backbone.Furthermore, the endothermic peak at 85 °C is attributed to vaporization of humidity or another organic resolvent. In other words, the quantity of HDPE-g-PMMA/Cloisite® 20 A nanocomposite in Tg and Tm can be gained at 127 °C and 183 °C. Of course, these quantities are scantly better than quantities in the HDPE-g-PMMA graft copolymer. These experimentals attribute due to the limitation of polymer chains adjoining to the silicate stratums that prohibit the sectional movement of the polymer backbone. Cloisite® 20 A stratums were dispersed in the polymer matrix at the nanoscale and solid interfacial strength made between the silicate stratums, and polymer backbone, might be limiting the movement of chain sections, as a result, we can see a growth in Tm and Tg. Characteristic TGA curves of HDPE, HDPE-g-MA, HDPE-g-PMMA, and HDPE-g-PMMA/Cloisite® 20 A nanocomposite are shown in Figure 6. As seen, HDPE was beginning to degrade in one stage at about 200–380 °C, and later on the loss rate became sluggish. The weight losses in (100–200 °C) are attributed to the vaporization of humidity or any organic solvent. The remaining sample at 550 °C for HDPE virtually is 2 wt.%. The HDPE-g-MA showed higher thermal stability, and the decomposition of this sample is started at up temperature value (270–385 °C).

The TGA thermogram of HDPE-*g*-PMMA copolymer exhibits two-stage weight loss processes; the first stage attributed to the decomposition of PMMA segments (230 to 320 °C), and the weight loss at up temperatures (320–380 °C) attributed to disintegration of HDPE backbone, that later on the loss rate became sluggish. It is necessary to explain that the decomposition of MA, also small molecules, occures during the first stage. The remaining amount of HDPE-*g*-PMMA sample at 550 °C is virtually 2 wt.%. As explained in the TEM image, this increase in the thermic attributes derived from the monotone dissipation of clay nanolayers in the HDPE-*g*-PMMA matrix, operate as obstacles for diminishing penetrance of fugacious degradation productions out of the matters.

Conclusions

A modified HDPE was successfully synthesized by the grafting of the MMA monomer using the RAFT technique. Furthermore, the result of an organo-modified clay (Cloisite® 20 A) on the thermal attributes of the obtained graft copolymer was considered by using DSC and TGA analysis. The synthesis of the HDPE-*g*-PMMA graft copolymer was verified using FTIR spectroscopy and SEM observation. The most significant benefits of exerted technics are grafted chain longitudes and controlled graft thickness. The HDPE-*g*-PMMA/Cloisite® 20 A nanocomposite by solution intercalation method by using 2 wt.% clay was constructed. The TEM and XRD research was disclosed a foliated structure for the synthesized nanocomposite. Thermic property outcomes by using DSC and TGA indicate that the synthesized HDPE-*g*-PMMA/Cloisite® 20 A nanocomposite has upper thermic constancy than HDPE-*g*-PMMA graft copolymer, just a minor extent (2wt. %) Cloisite® 20 A.

As a result, the synthesis of HDPE-*g*-PMMA graft copolymer, and HDPE-*g*-PMMA/Cloisite® 20 A nanocomposite can be excreted in numerous industrial fields basically sake of their minute manufacture costs. Also. The amended physicochemical attributes in comparison with pristine HDPE.

Supporting information summery

(1) Experimental section: In this section we give all of experimental that we used for Modification of high-density polyethylene through the grafting of methyl methacrylate and preparation its polymer/clay nanocomposites.

Acknowledgements

The writers state their sincere thanks from the University of Payame Noor for the sake of the financial support of this work.

Conflict of Interest

The authors declare no conflict of interest.

Data Availability Statement

The data that support the findings of this study are available from the corresponding author upon reasonable request.

Keywords: Clays · Graft copolymer · High-density polyethylene · Methyl methacrylate · Nanocomposite · Polymerization

[1] J. Wooster, J. Martin, *handbook of industrial polyethylene and technology*, Wiley, New York, **2017**, 1071.
[2] K. Yamamoto, H. Tanaka, S. Sakaguchi, *Polymer.* **2003**, *44*, 7661–7669.
[3] M. Ščetar, M. Kurek, K. Galić, *Cro. J. Food Sci. Technol.* **2010**, *2*, 32–48.
[4] R. K. Krishnaswamy, *Polymer.* **2005**, *46*, 11664–11672.
[5] P. J. DesLauriers, M. P. McDaniel, D. C. Rohlfing, R. K. Krishnaswamy, S. J. Secora, E. A. Benham, P. L. Maeger, A. R. Wolfe, A. M. Sukhadia, B. B. Beaulieu, *Polym. Eng. Sci.* **2005**, *45*, 1203–1213.
[6] Z. Chen, P. Fang, H. Wang, S. Wang, *J. Appl. Polym. Sci.* **2008**, *107*, 985–992.
[7] S. M. Desai, R. P. Singh, *Adv. Polym. Sci.* **2004**, *169*, 231–293.
[8] X. M. Zhang, S. Elkoun, A. Ajji, M. A. Huneault, *Polymer.* **2004**, *45*, 217–229.
[9] A. Roy, M. Joshi, B. S. Butola, A. K. Srivastava, *Polym. Compos.* **2018**, *39*, E366-E377.

[10] Y. Na, S. Dai, C. Chen, *Macromolecules.* **2018**, *51*, 4040–4048.
[11] C. Huang, J. He, R. Narron, Y. Wang, Q. Yong, *ACS Sustainable Chem. Eng.* **2017**, *5*, 11770–11779.
[12] H. Kaneyoshi, K. Matyjaszewski, *J. Appl. Polym. Sci.* **2007**, *105*, 3–13.
[13] S. Rutkowski, A. Zych, M. Przybysz, M. Bouyahyi, P. Sowinski, R. Koevoets, J. Haponiuk, R. Graf, M. R. Hansen, L. Jasinska-Walc, R. Duchateau, *Macromolecules.* **2017**, *50*, 107–122.
[14] X. Song, Q. Ma, Z. Cai, R. Tanaka, T. Shiono, R. B. Grubbs, *Macromol. Rapid Commun.* **2016**, *37*, 227–231.
[15] W. C. Chu, C. C. Cheng, B. P. Bastakoti, S. W. Kuo, *RSC Adv.* **2016**, *6*, 33811–33820.
[16] K. Nam, T. Iwata, T. Kimura, H. Ikake, S. Shimizu, T. Masuzawa, A. Kishida, *J. Appl. Polym. Sci.* **2014**, *131*, 40885 .
[17] Y. Zheng, J. Miao, F. Zhang, C. Cai, A. Koh, T. J. Simmons, S. A. Mousa, R. J. Linhardt, *Reac. Funct. Polym.* **2016**, *100*,142–150.
[18] J. Shin, X. Liu, N. Chikthimmah, Y. S. Lee, *Appl. Surf. Sci.* **2016**, *386*, 276–284.
[19] H. Oraby, M. M. Senna, M. Elsayed, M. Gobara, *J. Appl. Polym. Sci.* **2017**, *134*, 45410.
[20] R. Fleet, J. B. McLeary, V. Grumel, W. G. Weber, *Eur. Polym. J.* **2008**, *44*, 2899–2911.
[21] J. P. Kennedy, A. Vidal, *J. Polym. Sci. Polym. Chem. Ed.* **1975**, *13*, 2269–2276.
[22] M. Ciftci, M. Arslan, M. Buchmeiser, Y. Yagci, *ACS Macro Lett.* **2016**, *5*, 946–949.
[23] H. Kong, W. Li, C. Gao, D. Yan, Y. Jin, D. R. M. Walton, *Macromolecules.* **2004**, *37*, 6683–6686.
[24] D. Q. Fan, J. P. He, W. Tang, J. T. Xu, Y. L. Yang, *Eur. Polym. J.* **2007**, *43*, 26–34.
[25] J. Gupta, D. J. Keddie, C. Wan, D. M. Haddleton, T. McNally, *Polym. Chem.* **2016**, *7*, 3884–3896.
[26] R. G. Lopez, C. Boisson, F. D'Agosto, R. Spitz, F. Boisson, D. Bertin, P. Tordo, *Macromolecules.* **2004**, *37*, 3540–3542.
[27] R. G. Lopez, C. Boisson, F. D'Agosto, R. Spitz, F. Boisson, D. Gigmes, D. Bertin, *J. Polym. Sci. Polym. Chem. Ed.* **2007**, *45*, 2705–2718.
[28] Y. Zhao, L. Wang, A. Xiao, H. Yu, *Prog. Polym. Sci.* **2010**, *35*, 1195–1216.
[29] M. Barsbay, O. Güven, *Polymer.* **2013**, *54*, 4838–4848.
[30] R. Mohammad-Rezaei, B. Massoumi, M. Abbasian, M. Jaymand, *J. Polym. Res.* **2018**, *25*, 93.
[31] W. J. Wang, L. Pingwei, B. G. Li, Z. Shiping, *J. Polym. Sci. Polym. Chem. Ed.* **2010**, *48*, 3024–3032.
[32] F. Mahmoodzadeh, M. Abbasian, M. Jaymand, A. Amirshaghaghi, *Polym. Int.* **2017**, *66*, 1651–1661.
[33] M. Abbasian, M. judi, F. Mahmoodzadeh, M. Jaymand, *Polym. Adv. Technol.* **2018**, *29 (12)*, 3097–3105.
[34] B. Massoumi, S. V. Mousavi-Hamamlu, A. Ghamkhari, M. Jaymand, *Polym.-Plast. Technol. Eng.* **2017**, *56*, 873–882.
[35] B. Høgsaa, E. H. Fini, J. D. C. Christiansen, A. Hung, M. Mousavi, E. A. Jensen, F. Pahlavan, T. H. Pedersen, C. G. Sanporean, *Ind. Eng. Chem. Res.* **2018**, *57*, 1213–1224.
[36] T. O. Morgen, M. Krumova, H. Luttikhedde, S. Mecking, *Macromolecules.* **2018**, *51*, 4118–4128.
[37] Z. Zhou, H. Zhai, W. Xu, H. Guo, C. Liu, W. P. Pan, *J. Appl. Polym. Sci.* **2006**, *101*, 805–809.
[38] M. Abbasian, F. Mahmoodzadeh, *J. Elastomers Plast.* **2017**, *49*, 173–193.
[39] M. Abbasian, M. Pakzad, M. Amirmanesh, *Polym. Compos.* **2017**, *38*, 1127–1134.
[40] S. G. Karaj-Abad, M. Abbasian, M. Jaymand, *Carbohydr. Polym.* **2016**, *152*, 297–305.
[41] M. Abbasian, M. Jaymand, S. E. Shoja Bonab, *J. Appl. Polym. Sci.* **2012**, *125*, E131-E140.
[42] M. Jaymand, *Polym. J.* **2011**, *43*, 901–908.
[43] M. Jaymand, *Polym. J.* **2011**, *43*, 186–193.

Submitted: November 27, 2021
Accepted: March 1, 2022